Journal Name

Dynamic Article Links ►

Cite this: DOI: 10.1039/c0xx00000x

www.rsc.org/xxxxxx

ARTICLE TYPE

A Fluorescent Arg–Gly–Asp (RGD) Peptide - Naphthalenediimide (NDI) Conjugate for Imaging Integrin $\alpha_v\beta_3$ *In Vitro*

Zhiyuan Hu[#¶*], Rory L. Arrowsmith[¶], James A. Tyson[¶], Vincenzo Mirabello[¶], Haobo Ge[¶], Ian M. Eggleston[§], Stan W. Botchway[‡], G. Dan Pantos[¶*], Sofia I. Pascu[¶*]

Received (in XXX, XXX) Xth XXXXXXXXX 20XX, Accepted Xth XXXXXXXXX 20XX

DOI: 10.1039/b000000x

We have developed a fluorescent peptide conjugate (TrpNDIRGDfK) based on the coupling of cyclo(RGDfK) to a new tryptophan-tagged amino acid naphthalenediimide (TrpNDI). Confocal fluorescence microscopy coupled with fluorescence lifetime imaging (FLIM) mapping, single and two-photon fluorescence excitation, lifetime components and corresponding decay profiles were used as parameters able to investigate qualitatively the cellular behavior regarding the molecular environment and biolocalisation of TrpNDI and TrpNDI-RGDfK in cancer cells.

Tumor angiogenesis is the process of growing new blood vessels that can assist cancerous growths through the supply of nutrients and oxygen as well as removing waste products.[1] Angiogenesis is an important feature of the spread of a tumor, given that single cancer cells can escape into blood vessels and can also be transported to distant sites,[2] thus generating secondary tumors. Angiogenesis is a potential target for combating cancer as it plays a key role in tumor metastasis and growth. The use of specific compounds that may inhibit new blood vessels formation at the tumor site may help to switch off the metastasis, but their intimate behavior at the cellular level remains a matter of intense investigations: as such, the $\alpha_v\beta_3$ integrin peptide is one of the most important molecular markers involved in the mechanism of cell adhesion to the extracellular matrix (ECM). The integrin is highly expressed during angiogenesis and plays an important role in transferring signals from the extra-cellular environment to the intracellular compartment.[3] The $\alpha_v\beta_3$ integrin is absent in resting endothelial cells and most normal organ systems, rendering it a potential target for anti-angiogenic cancer therapy. Tumor progression and metastasis of breast cancer, glioma, melanoma and ovarian carcinoma are all linked to $\alpha_v\beta_3$ integrin overexpression during tumor angiogenesis. It has been found that several proteins such as vitronectin, fibrinogen and fibronectin can bind to $\alpha_v\beta_3$ integrin *via* the same amino acid sequence arginine-glycine-aspartic acid, or RGD.[4] It has been shown that cyclo(RGDfK) is one of the most prominent structures for development of molecular imaging agents for the assessment of $\alpha_v\beta_3$ expression. This pentapeptide, cyclo(-Arg-Gly-Asp-DPhe-Val-), was developed by Kessler and co-workers to show high affinity and selectivity for $\alpha_v\beta_3$ integrin.[5]

We, and others, have studied the supramolecular chemistry of functionalised naphthalene diimides: NDI molecules have attracted considerable attention recently because of excellent electron accepting properties and solubility in biocompatible media as well as organic solvents [6-7]. NDIs and their derivatives are flat, aromatic molecules which have fluorescent properties, suitable for single- and two-photon cellular imaging and are easily functionalisable with amino acids.[7] These make NDI derivatives attractive candidates as building blocks for optical imaging probes, particularly as NDIs have strong absorption and fluorescence emissions in the visible and near-IR wavelengths. Previous work on aminoacid-functionalised NDIs showed that, despite quantum yields that rather low in aqueous media (less than 0.005 with respect to [Ru(bipy)$_3$PF$_6$]' likely due to non-radiative decay pathways emerging from aromatic stacking and internal hydrogen bonds)[8], such materials are taken up by cancer cells in preference with respect to healthy cells. Here, the first NDI-peptide imaging probe incorporating a cancer specific targeting peptide (cyclic RGDfK) and an amino acid (L-Trp) was designed and synthesised in two simple synthetic steps through the EDC-mediated coupling to the strongly fluorescent tryptophan-NDI, which emits broadly in both single- and two-photon excitation with maxima above 500 nm.

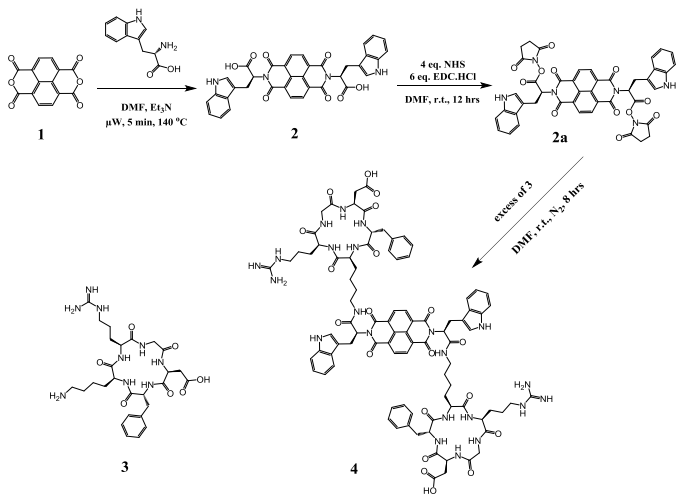

Scheme 1. Synthesis of tryptophan-NDI-RGDfK, compound **4**

To shed light into the fate of bio/medical imaging probes in a cellular environment, the uptake of the new compounds **2** and **4** shown in Scheme 1 was investigated using Fluorescence Lifetime Imaging Microscopy (FLIM) coupled with multiphoton confocal

fluorescence microscopy: this combination of methods, together with MTT assays already provided reliable means to probe directly the environmental effects upon uptake and biolocalisation of aromatic compounds as probes inside living cells.[7b, 8-9]

The cyclo-(RGDfK) was chosen in particular for the potential to selectively bind to prostate cancer cells that overexpress the specific target receptor. Furthermore, the NDIs plus cyclo-(RGDfK) conjugates were used to image cancer cells *in vitro*.

A series of purpose-made RGDfK peptides were synthesised on a laboratory scale using a standard Fmoc solid phase synthesis protocol, as described in ESI. The resulting cyclic peptide **3** was successfully isolated and characterised by ^{1}H NMR in d^6-DMSO (including NOESY to verify cyclisation), ESI/MS, MALDI and HPLC. A new compound, tryptophan substituted NDI (TrpNDI, compound **2**) was synthesised from L-Tryptophan and 1,4,5,8-naphtalenetetracarboxylic dianhydride (**1**), using a rapid and straightforward microwave-assisted method (Scheme 1), in almost quantitative yield. The molecular structure and supramolecular self-assembly of TrpNDI (**2**) was determined in the solid state by single crystal X-ray crystallography (Figure 1). Crystals suitable for analysis were grown from DMSO and synchrotron single crystal X-ray diffraction data was obtained for **2**. The molecules are held together in a hydrogen bonded network formed between the tryptophan NH of one molecule and the carboxylic carbonyl C=O from neighbouring molecules (N1···O2 2.868 Å, 162.3°; N4···O7 2.862 Å, 168.4°). This supramolecular structure is further reinforced by π-π donor-acceptor interactions between the tryptophan residue and the NDI core (avg. π···π distance 3.233Å, with a 5.9° angle between the two avg. π planes). The carboxylic OH is involved in hydrogen bond interactions with the solvent molecules (DMSO and H_2O). Crystal data and structure refinement parameters are included in ESI.

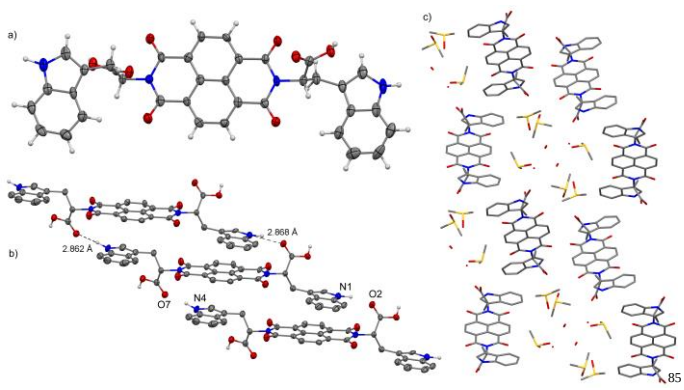

Figure 1. Molecular structure of Compound **2**: (**a**) Side and (**b**) crystal unit cell packing views of TrpNDI where all hydrogen atoms and a disordered solvent molecule (DMSO) have been removed for clarity. (**c**) a view along the a axis rotated by 90° in the b/c plane showing disordered H_2O and DMSO solvating molecules.

With compound **2** in hand, the corresponding NDI-RGDfK conjugate (TrpNDI-RGDfK, **4)** was synthesised by coupling the EDC-functionalised TrpNDI intermediate (compound **2a**, described in ESI) to the amino group of lysine residue of the deprotected cyclic peptide RGDfK (compound **3**, as shown in Scheme 1 and described in ESI). The novel NDI-peptide conjugate (TrpNDI-RGDfK) was purified and isolated by semi preparative-HPLC on a milligram scale and characterised by MALDI mass spectrometry (given in ESI).

The quantum yield of TrpNDI (**2**) was determined to be 0.002 in DMSO, with fluorescein in aqueous 0.1 M NaOH as the reference[10]. This was in line with that found for related NDIs in aqueous environments and, since earlier studies on NDIs and related molecules showed that this does hamper the cellular tracing by multiphoton confocal fluorescence imaging, fluorescence lifetime imaging microscopy (FLIM) and confocal laser scanning microscopy were utilised as the imaging tools of choice for the investigations into the probe behavior in living cells. Furthermore, MTT assays (ESI) showed that at concentrations of ca. 100 μM both compounds **2** and **4** are biocompatible within 48 h observation time towards both FEK-4 (a healthy cell line) and PC-3 (prostate cancer cell line). ESI describes in full the results of the cellular viability assays. The stability of **4** with respect to decomposition and the retention of corresponding *in vitro* fluorescence emissions were probed in living cells for both TrpNDI (**2**) and TrpNDI-RGDfK (**4**). In order to detect TrpNDI (**2**) and its RGDfK derivative (**4**) inside cancer cells, FLIM was used here for mapping the lifetime of the fluorophores' emission and also to shed light upon their cellular biodistribution: this was found, in control experiments (described in ESI) to be significantly removed from cellular autofluorescence. Interestingly, unlike related NDIs, compounds **2** and **4** do not localise in the cells' nuclei but throughout the cytoplasm. Figures 2 and 3 show single photon confocal laser scanning microscopy (CLSM) images of TrpNDI (**2**) and TrpNDI-RGDfK (**4**) in PC-3 cells (λ_{ex} = 543 nm). TrpNDI (**4**) shows emission upon exciting at either 405 nm, 488 nm and 543 nm, but TrpNDI-RGDfK only shows emission after exciting at 543 nm alone. This strongly suggests that following the tagging of **2** with two c(RGDfK) units, the incorporation of this peptide narrows the excitation wavelength range necessary to bypass the cellular autofluorescence and to trace compound **4** *in vitro*.

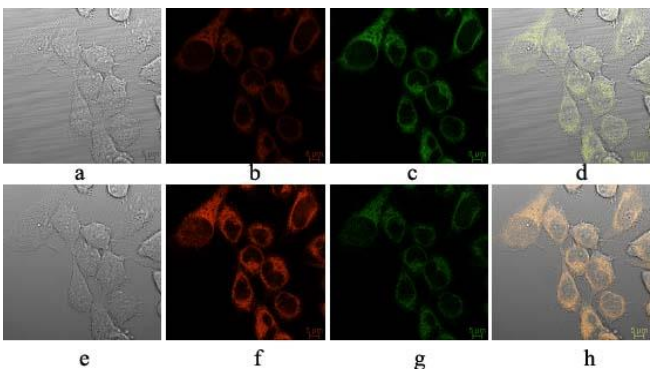

Figure 2. Single-photon laser-scanning confocal microscopy of PC-3 cells incubated for 25 min. at 37 ºC with Compound **2** (100 μM in 1: 99 % DMSO: serum free medium): (**a-d**) (λ_{ex} = 405 nm, broad observed weak emission between 515-530 nm); (**e-h**) (λ_{ex} = 488 nm, broad observed emission both in the red 605-675 nm and green 515-530 nm channels). Micrographs **a** and **e** show the bright-field images, confirming a 'healthy' cellular morphology within this experiment time; **d** and **h** represent overlays of the micrographs (**a-b-c**) and (**e-f-g**) respectively. Scalebar: 5 μm.

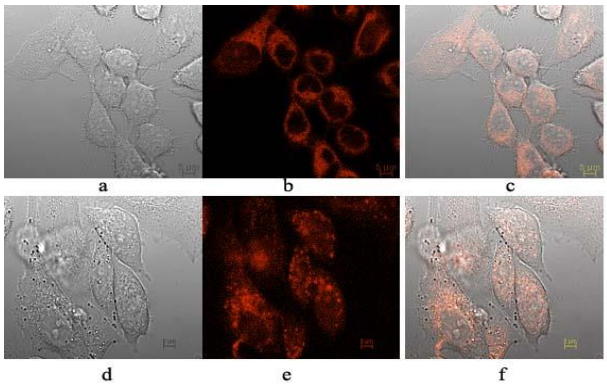

Figure 3. Single-photon laser-scanning confocal microscopy (λ_{ex} = 543 nm, observed emission: 605-675 nm) of PC-3 cells incubated for 25 mins at 37 °C with: (**a-c**) Compound **2** (100 μM in 1: 99 % DMSO: serum free medium); (**d-f**): Compound **4** (100 μM in 1: 99 % DMSO: serum free medium). Scalebar 5 μm. The biolocalisation of **2** is uniform throughout the cytoplasm whereas that of **4** occurs mainly in punctuated, vesicular regions in the cytoplasm.

Two photon imaging experiments were carried out given that standard dyes co-staining assays were not conclusive in pinpointing specific organelles for dyes' biolocalisation. To investigate the effect of the environment on the new probes, lifetime measurements were recorded using time-correlated single photon counting with an excitation wavelength of 810 nm and the emission measured at 360-580 nm both in solutions and in living cells. The solution measurements of TrpNDI and TrpNDI-RGDfK were carried out in DMSO solutions with concentration of 10 mM (stock) and 100 μM. Figure 4 shows an overlay of the two-photon excitation lifetime decay curves for Compounds TrpNDI **2** and TrpNDIRGDfK **4** in solution. Lifetime components data were processed using SPCImage analysis software (Becker and Hickl, Germany) or Edinburgh Instruments F900 TCSPC analysis software. The data profile includes the goodness of fit of the decay curves as χ^2, and the lifetime of each component and their weighting of each component are given in Tables 1 and 2. The χ^2 value of 1.0 means an optimal single exponential fit of this measurement. If the χ^2 value is more than 1.3 there is an incomplete single exponential fit of this measurement. High χ^2 values (>1.5) mean either significant noise within the TCSPC setup (electronics and/or excitation source) or more than one component decay profile.

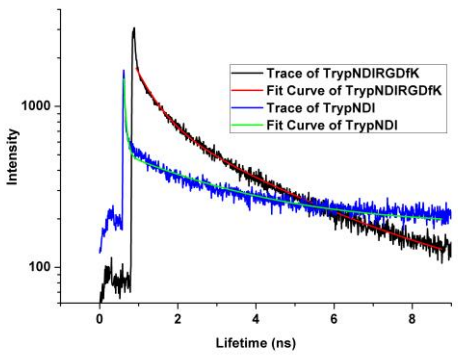

Figure 4. Two-photon time-correlated single photon counting: fluorescence decay traces and corresponding fitted curves for the lifetime determinations (λ_{ex} = 810 nm, TrpNDI **2**, TrpNDIRGDfK **4**, 10 mM, pure DMSO, 5.7 mW).

Both TrpNDI **2** and TrpNDI-RGDfK **4** (10 mM stock solutions in DMSO, 2P excitation 810 nm) were found to decay as two component systems, with minor components (τ_2) in the order of several nanoseconds and major components (τ_1) in the order of several hundred picoseconds (Table 1). In DMSO, at 100 μM Compound **2** was also found to decay as a three component system, with a τ_1 of 0.1 ns (50%), with a τ_2 of 0.7 ns (22.8%) and a τ_3 of 3.2 ns (27.2%), the χ^2 was 1.18. The TSPC spectrum of TrpNDI-RGDfK displays a very close decay behavior to that of TrpNDI (Table 1, Figure 4 and ESI) and in both cases evidence of some aggregation (in line with the X-ray structure observations, Figure 1) may account for the extremely short lifetime components present.

Next, living PC-3 cells were plated on Petri dishes incorporating a glass cover slip and allowed to adhere for 12 h. Background lifetime readings were recorded using fluorescence lifetime imaging microscopy (FLIM) before the addition of compound. The Petri dishes containing the cells were then mounted on the microscope stage and kept at 37 °C during imaging, which was performed immediately.

Table 1. Lifetime decay constants for compounds **2** and **4** point decay recorded in pure DMSO solutions (10 mM)

Compounds	τ_1 / ns	A_1 %	τ_2 / ns	A_2 %	χ^2
2	0.6	45.9	2.8	54.1	1.2
4	0.6	55.4	2.9	44.6	1.0

Compounds **2** and **4** were dissolved in DMSO and added to the cells to achieve a final concentration of dye of 100 μM in EMEM medium containing 1% DMSO (*v/v*). Cell uptake was monitored after 20 min incubation. Furthermore, precursor compound **2** was also incubated at a final concentration of 500 μM and 5 % DMSO (*v/v*) *(ESI)*. Measurements were recorded for the whole field of view. The FLIM images obtained for TrpNDI (**2**) and its RGDfK derivative **(4)** are displayed in Figures 5 and 6, including an intensity map showing spatial variations in fluorescence emission, the lifetime map displaying the distribution of different fluorescence decay lifetimes throughout the cellular cytoplasm and the profiles of the corresponding lifetime distributions. The excited state lifetime data (Table 2) show that compounds **1**, **2** and **4** have two lifetime components: a major component A1 for (τ_1) and a minor component A2 for (τ_2). Compound **2** possessed lifetime components in PC-3 cells closely matched those observed in DMSO solution, with compound **1** displaying a τ_1 and τ_2 in a cellular environment similar to the τ_2 and τ_3 found in DMSO. Interestingly in PC-3 cells both lifetime components were shorter than observed in solution, indicating less stable excited state in the cellular environment. Furthermore, a control in PC-3 cells showed entirely different lifetime components from the case when 2 or 4 were incubated with this cell line (Table 2). This confirms that the compounds do indeed enter the cells, and in line with single photon CLSM measurements, both **2** and **4** predominantly localise within the cytoplasm with negligible nuclear uptake, unlike the related iodine-fundtionalised L-phenyl alanine NDI reported earlier.[8] Interestingly, although both **2** and **4** are biocompatible with the living cells used hereby within the imaging experiments' timescales, they exhibit different fluorescence lifetime values, but which are comparable with those resulting from the solution experiments and also show clearly distinct cellular distributions in vitro. This is not surprising given the presence of the RDG targeting peptide in **4**, molecular size and shape differences and the fact that compound **4** is more likely than **2** to form large lipophilic cations upon protonation.

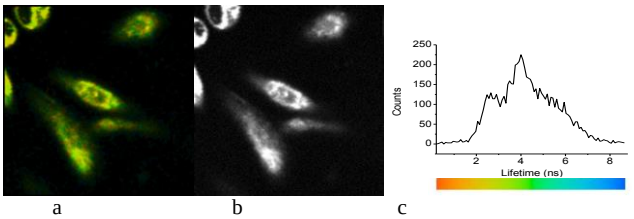

a b c

Figure 5. Two-photon laser confocal fluorescence with λ_{ex} = 810 nm. (**a**) Typical micrograph of PC-3 cells incubated for 20 min at 37 °C with compound **2** (100 μM in 1: 99 % DMSO: EMEM showing compound **2** located throughout in cytoplasm, lifetime mapping; (**b**) 2-photon fluorescence emission intensity image and (**c**) corresponding average τ lifetime distribution curve and lifetime scale-bar.

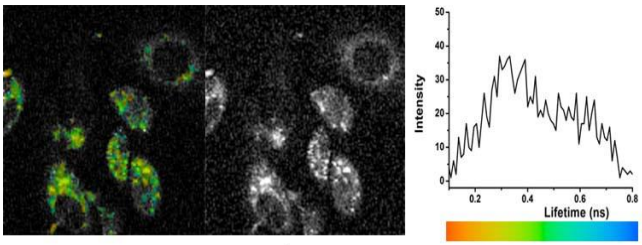

a b c

Figure 6. Two-photon laser confocal fluorescence with λ_{ex} = 810 nm. Typical micrograph of PC-3 cells incubated for 20 min at 37 °C with compound **4** (100 μM in 1: 99 % DMSO: EMEM showing compound **4** mainly located in vesicular regions in the cytoplasm: lifetime mapping (**a**), intensity image (**b**), and corresponding average τ lifetime distribution curve and lifetime scale-bar (**c**).

Table 2. Typical lifetime decay constants for compounds **2** and **4** evaluated in cellular regions showing uptake in PC-3 cancer cells from Figures 5 and 6, as well as Control (ESI). Individual lifetime components and their contributions are given.

Compound	τ_1 / ns	FHHM / ns	A_1 %	τ_2 / ns	FHHM / ns	A_2 %	χ^2
2	1.0	0.5	80.1	4.0	2.3	20.1	1.16
4	0.3	0.1	75.7	1.9	0.73	24.3	1.00
Control	1.3	0.4	79.8	5.2	2.3	20.2	1.29

In summary, we developed a new type of molecular imaging agent based on the cancer targeting peptide cRGDfK coupled to an aminoacid functionalised NDI. Fluorescence lifetime mapping, fluorescence intensity profile, lifetime components and lifetime decay profile were all employed together with MTT assays to demonstrate the integrity of these molecular imaging agents in cancer cells (PC-3 cells) and their biocompatibility against cancerous (PC-3) as well as non-cancerous (FEK-4) cell lines. The close similarity between the lifetimes measured for these compounds in solution and those determined within cells confirm the cellular uptake of such molecules, and offer compelling evidence that these are different with respect to those of free, untreated living cells. These measurements confirm the integrity of such NDI compounds within living cells and their cytoplasmic distribution.

We thank the University of Bath and EPSRC for studentships (ZH, JAT, RLA) and the EC (ERC Consolidator Grant O2SENSE), Royal Society, MRC and STFC for financial support. We also thank the EPSRC Mass Spectrometry Service at Swansea for assistance, STFC for funding the SRS crystallography work, Mr Colin Wright (Nikon Bioimaging Ltd), Prof. Jon Dilworth and Mr Colin Sparrow (University of Oxford) and Dr John Warren (University of Manchester) for training and helpful discussions.

Notes and references

[#] *State Key Lab of Heavy Oil Processing, China University of Petroleum-Beijing, No 18 Fuxue Road, 102249, Beijing,*
[¶]*Department of Chemistry, University of Bath, Claverton Down, BA2 7AY, UK*
[§]*Department of Pharmacy and Pharmacology, University of Bath, Claverton Down, BA2 7AY, UK*
[‡]*Central Laser Facility, Rutherford Appleton Laboratory, Research Complex at Harwell, STFC, Didcot, OX11 0QX, UK*
[*]*Corresponding authors: Dr. S. I. Pascu, E-mail: s.pascu@bath.ac.uk; Dr G.D.Pantos, g.d.pantos@bath.ac.uk, Dr. Zhiyuan Hu, E-mail: zh209@cup.edu.cn*

† Electronic Supplementary Information (ESI) available. [Xray data for TrpNDI, analytical and semi-preparative HPLC data, Synthesis of the RGDfK peptide, Cell culture and control experiments, MTT assays, ESI-MS and MALDI spectra and HPLC are included in supplementary materials.]. See DOI: 10.1039/b000000x/

1 T. Acker and K. H. Plate, *J. Mol. Med.*, 2002, **80**, 562.
2 (a) C. D. Gadaleta and G. Ranieri, *Crit. Rev. Oncol. Hemat.*, 2011, **80**, 40; (b) A. Lequerrec, D. Duval and G. Tobelem, *Baillieres Clin. Haem.*, 1993, **6**, 711; (c) K. A. Rmali, M. C. A. Puntis and W. G. Jiang, *Colorectal Disease*, 2007, **9**, 3.
3 V. Pedchenko, R. Zent and B. G. Hudson, *J. Biol. Chem.*, 2004, **279**, 2772.
4 (a) M. A. Buerkle, S. A. Pahernik, A. Sutter, A. Jonczyk, K. Messmer and M. Dellian, *Brit. J. Cancer*, 2002, **86**, 788; (b) S. Cressman, Y. Sun, E. J. Maxwell, N. Fang, D. D. Y. Chen and P. R. Cullis, *International Journal of Peptide Research and Therapeutics*, 2009, **15**, 49; (c) M.Fani, D. Psimadas, C. Zikos, S. Xanthopoulos, G. K. Loudos, P. Bouziotis and A. D. Varvarigou, *Anticancer Res.*, 2006, **26**, 431; (d) V. I. Romanov and M. S. Goligorsky, *Prostate*, 1999, **39**, 108.
5 (a) M. A. Dechantsreiter, E. Planker, B. Matha, E. Lohof, G. Holzemann, A. Jonczyk, S. L. Goodman and H. Kessler, *J. Med. Chem.*, 1999, **42**, 3033; (b) R. Haubner, H. J. Wester, W. A. Weber, C. Mang, S. I. Ziegler, S. L. Goodman, R. Senekowitsch-Schmidtke, H. Kessler and M. Schwaiger, *Cancer Res.*, 2001, **61**, 1781; (c) U. Hersel, C. Dahmen and H. Kessler, *Biomaterials*, 2003, **24**, 4385.
6 M. Albota, D. Beljonne, J. L. Bredas, J. E. Ehrlich, J. Y. Fu, A. A. Heikal, S. E. Hess, T. Kogej, M. D. Levin, S. R. Marder, D. McCord-Maughon, J. W. Perry, H. Rockel, M. Rumi, C. Subramaniam, W. W. Webb, X. L. Wu and C. Xu, *Science*, 1998, **281**, 1653.
7 (a) S. Asir, A. S. Demir and H. Icil, *Dyes and Pigments*, **84**, 1; (b) H. E. Katz, J. Johnson, A. J. Lovinger and W. J. Li, *J. Am. Chem. Soc.*, 2000, **122**, 7787.
8 Z. Hu, G. D. Pantos, N. Kuganathan, R. L. Arrowsmith, R. M. J. Jacobs, G. Kociok-Koehn, J. O'Byrne, K. Jurkschat, P. Burgos, R. M. Tyrrell, S. W. Botchway, J. K. M. Sanders and S. I. Pascu, *Advanced Functional Materials*, 2012, **22**, 503.
9 P. A. Waghorn, M. W. Jones, M. B. M. Theobald, R. L. Arrowsmith, S. I. Pascu, S. W. Botchway, S. Faulkner and J. R. Dilworth, *Chem. Sci.*, 2013, **4**, 1430.
10 A. T. R. Williams, S. A. Winfield and J. N. Miller, *Analyst*, 1983, **108**, 1067.